Electronic Supplementary Information (ESI)

$LiTi_2(PO_4)_3$/reduced graphene oxide nanocomposite with enhanced electrochemical performance for lithium-ion batteries

Ha-Kyung Roh,[a] Hyun-Kyung Kim,[a] Kwang Chul Roh,*[b] and Kwang-Bum Kim*[a]

[a] *Department of Materials Science & Engineering, Yonsei University, 50 Yonsei-ro, Seodaemun-gu, Seoul 120-749, Republic of Korea. E-mail: kbkim@yonsei.ac.kr*

[b] *Energy Efficient Materials Team, Energy & Environmental Division, Korea Institute of Ceramic Engineering & Technology, 233-5 Gasan-dong, Guemcheon-gu, Seoul 153-801, Republic of Korea. E-mail: rkc@kicet.re.kr*

Supplementary Table

	wt.% of elements from elemental analysis		
$LiTi_2(PO_4)_3$/rGO	Carbon	Hydrogen	Nitrogen
	24.1	0.02	0.73

Table S1. CHNS elemental analysis of the $LiTi_2(PO_4)_3$/rGO nanocomposite.

Supplementary Figures

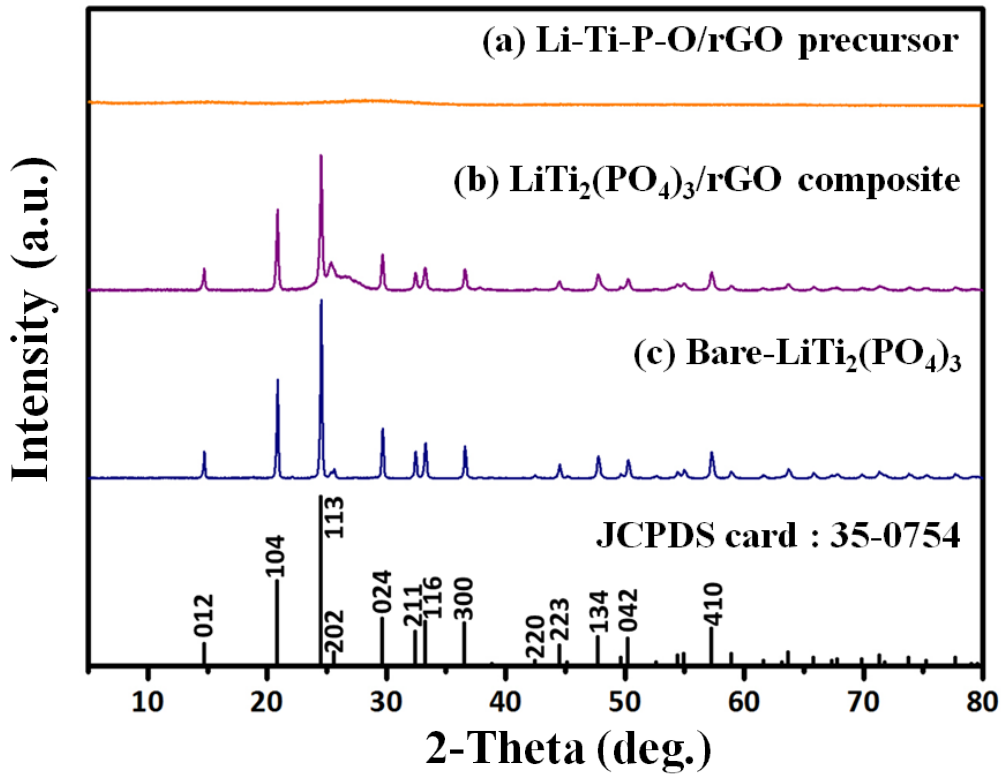

Figure S1. X -ray diffraction patterns of (a) the amorphous phase of the Li–Ti–P–O/rGO precursor, (b) the $LiTi_2(PO_4)_3$/rGO nanocomposite, (c) the bare $LiTi_2(PO_4)_3$ prepared by the Pechini sol-gel method. Both the $LiTi_2(PO_4)_3$ samples, prepared either by the microwave-assisted solvothermal method or the Pechini sol-gel method, were phase-pure according to their XRD patterns. The XRD patterns corresponding to standard NASICON-structured $LiTi_2(PO_4)_3$ (JCPDS card no. 35-0754) are provided for reference.[1-4]

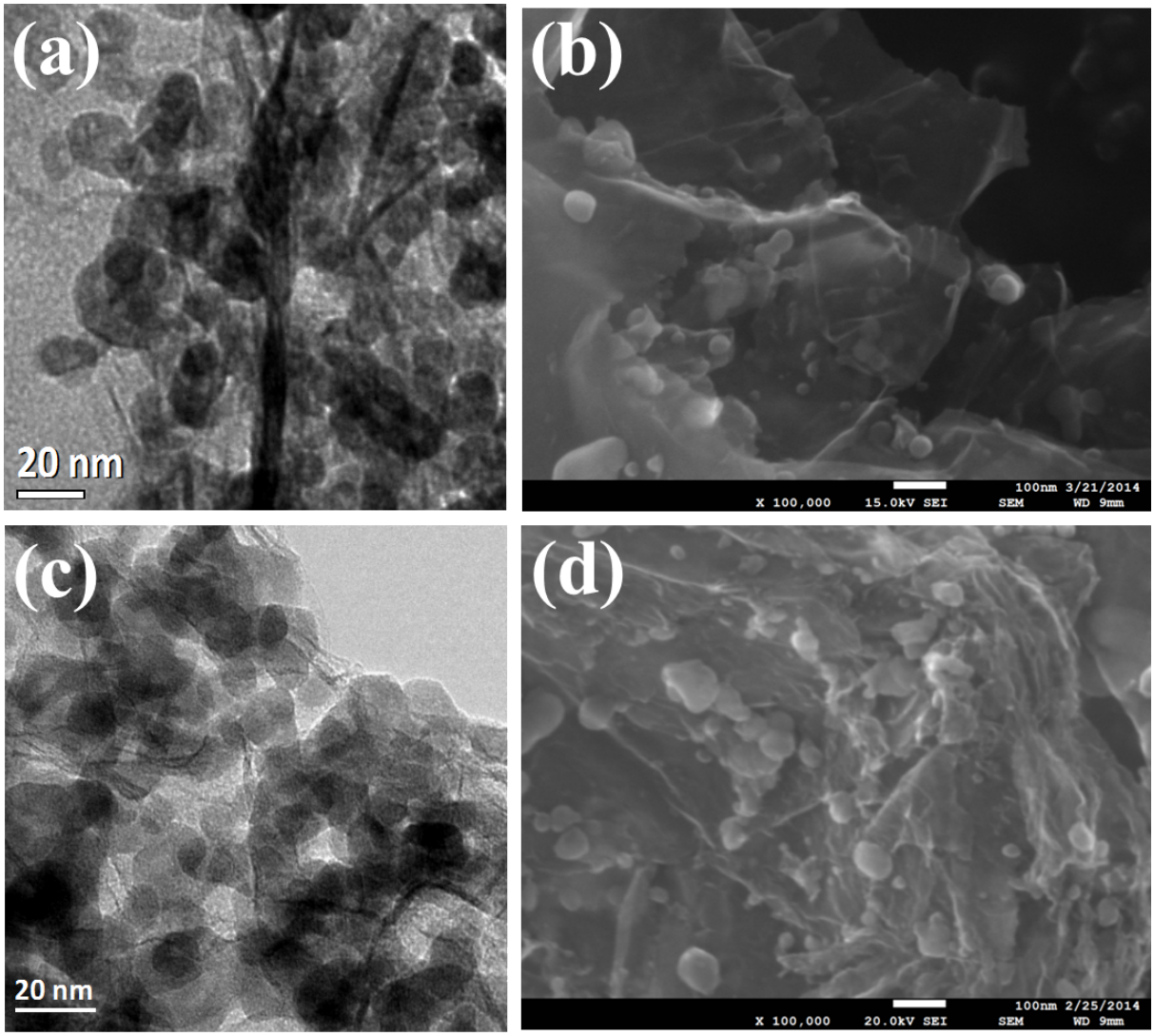

Figure S2. (a) TEM and (b) SEM images of the Li–Ti–P–O/rGO precursor and (c) TEM and (d) SEM images of the $LiTi_2(PO_4)_3$ nanoparticles after calcination. Both before and after calcination, $LiTi_2(PO_4)_3$ nanoparticles with a narrow size distribution of ~40 nm are firmly anchored on the rGO surface with no indication of morphological changes.

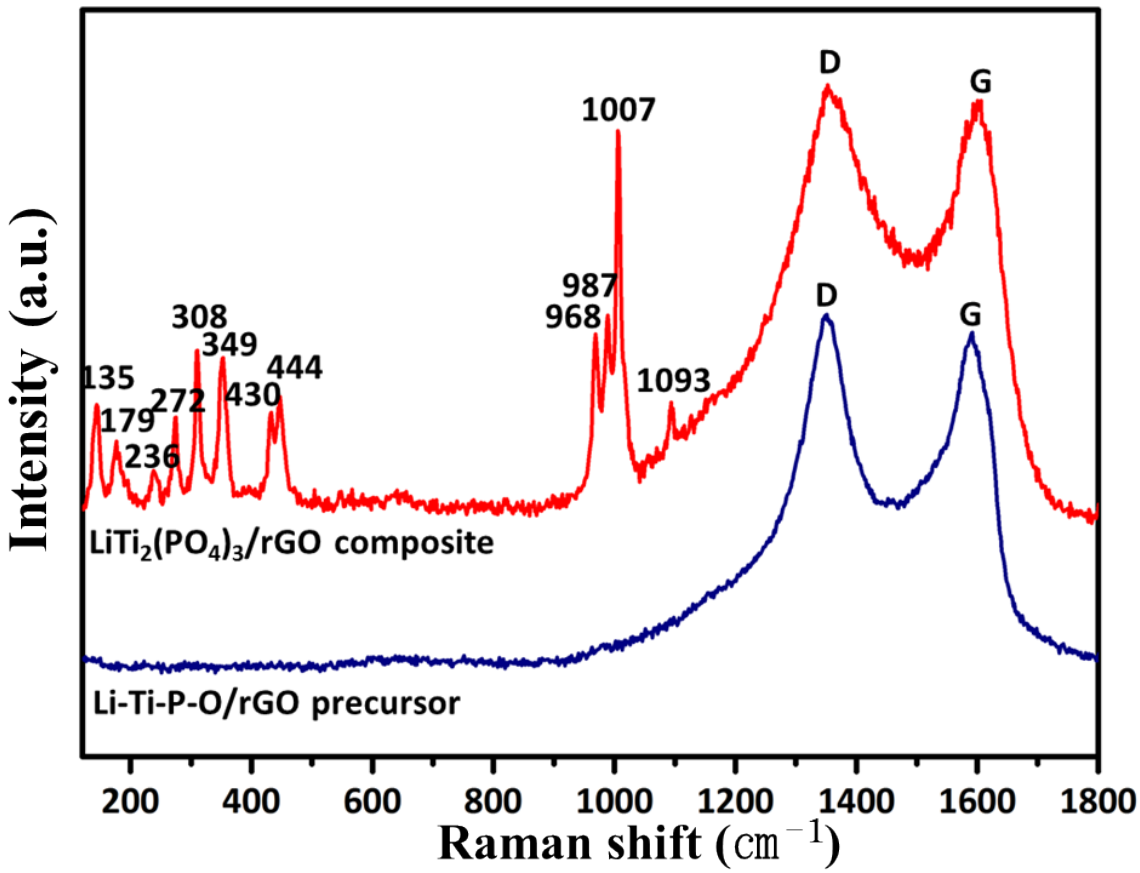

Figure S3. Raman spectrum of $LiTi_2(PO_4)_3$ in the $LiTi_2(PO_4)_3$/rGO nanocomposite. The Raman spectrum showed four characteristic peaks at 968, 987, 1007 and 1093 cm^{-1}. The bands at 135, 272 cm^{-1} are assigned to translational vibrations of the Ti^{4+} ions, while the bands at 179, 236, 308, 349, 430, 444 cm^{-1} are assigned to modes that are predominantly associated with $(PO_4)^{3-}$ motions. These Raman-allowed phonon peaks are the fingerprints of the NASICON-structure, which confirm the formation of phase-pure NASICON-structured $LiTi_2(PO_4)_3$in the nanocomposite. The Raman spectra corresponding to standard $LiTi_2(PO_4)_3$ are provided for reference.[5-7]

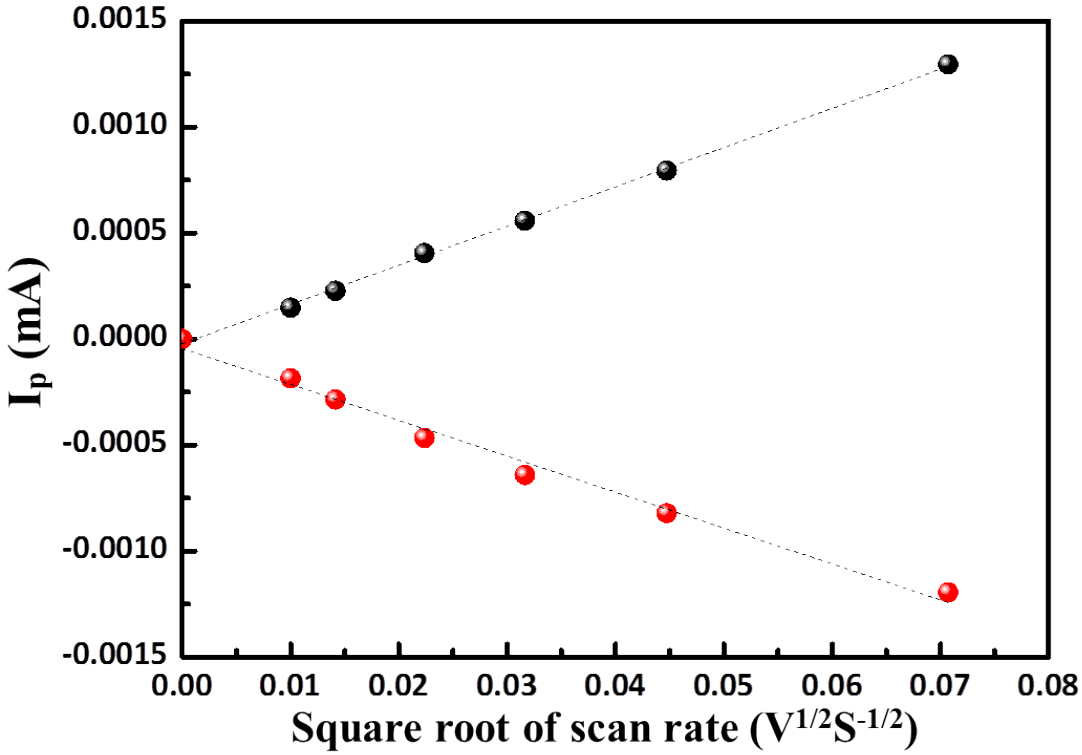

Figure S4. Linear plot of the relationship between the peak current (I_p) and the square root of the scan rate ($\nu^{1/2}$) for both the anodic and cathodic scans of $LiTi_2(PO_4)_3$/rGO nanocomposite.

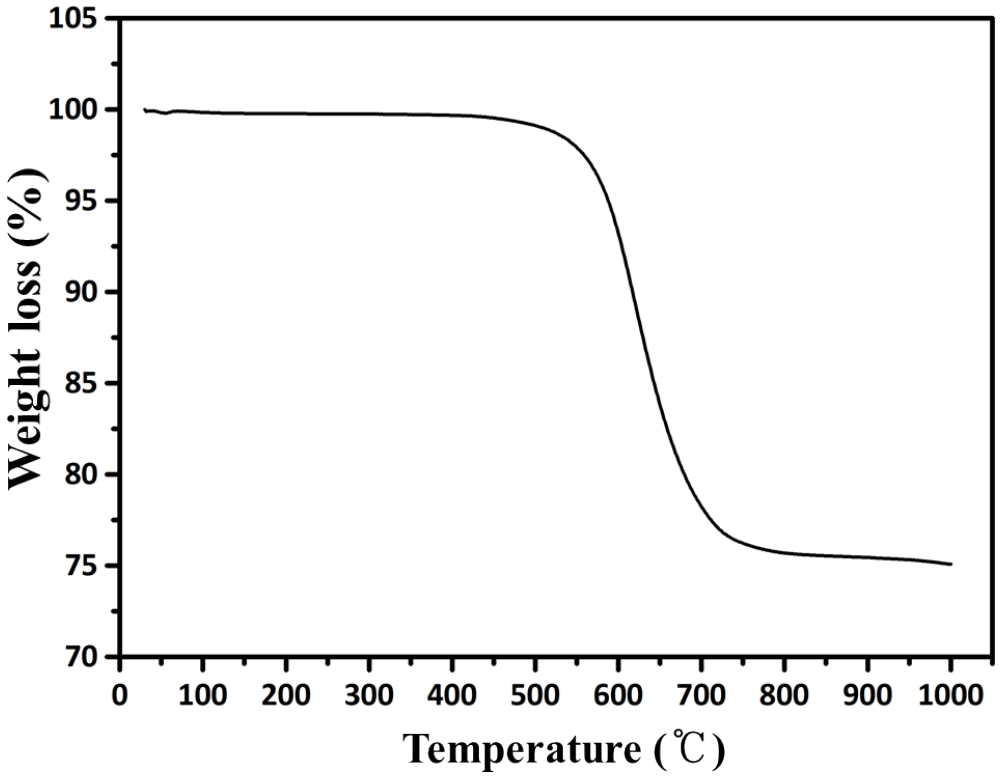

Figure S5. TGA plots of the $LiTi_2(PO_4)_3$/rGO nanocomposite, heated at10 °C min^{-1} from room temperature to 1000 °C under air flow. From these thermogravimetric data, the loading of $LiTi_2(PO_4)_3$ in the $LiTi_2(PO_4)_3$/rGO nanocomposite was determined to be 75 wt%.

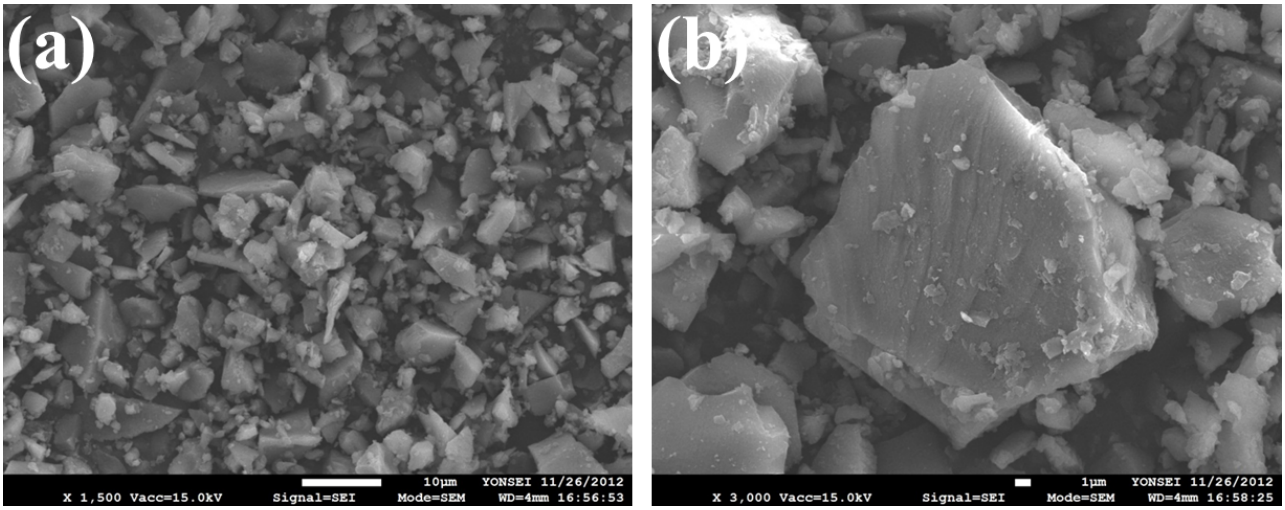

Figure S6. SEM images of bare $LiTi_2(PO_4)_3$ prepared by the Pechini method. The resulting bare $LiTi_2(PO_4)_3$ particles are mostly of submicron sizes, and few micron-sized particles have agglomerated in the absence of rGO.

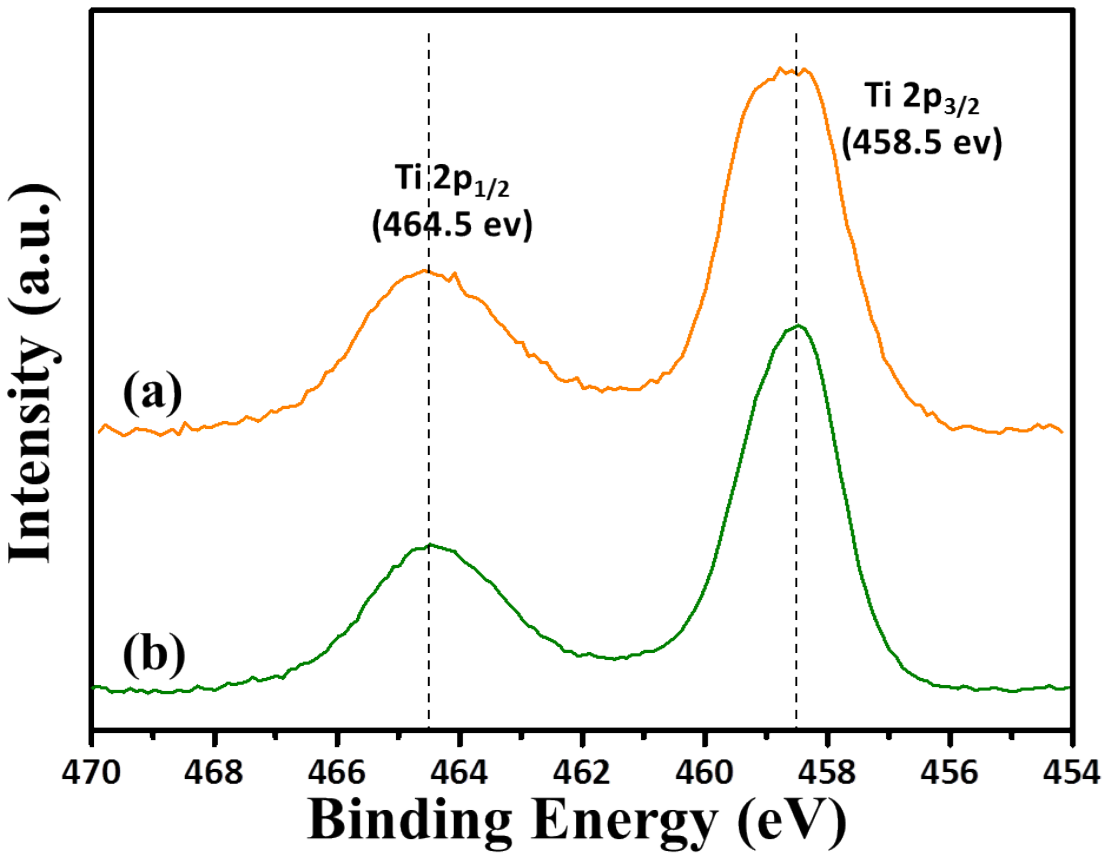

Figure S7. XPS Ti 2p spectra of the (a) Li-Ti-P-O/partially reduced GO precursor and (b) $LiTi_2(PO_4)_3$/rGO nanocomposite, which indicates before and after calcination. As shown in Fig. S7, there are two pairs of Ti 2p peaks with binding energies of 458.5 eV and 464.5 eV, attributed to Ti $2p_{3/2}$ and Ti $2p_{1/2}$, respectively, which typically Ti^{4+} in an octahedral environment.[8, 9] As shown in Fig. S7(b), the Ti 2p signals of the $LiTi_2(PO_4)_3$/rGO composite calcined under inert gas at 800 °C for 10 h only corresponding to Ti^{4+} and there are no peaks that belong to Ti^{3+}, similar to Fig. S7(a).

References

1. V. Aravindan, W. Chuiling and S. Madhavi, *RSC Advances*, 2012, 2, 7534-7539.
2. J. Y. Luo and Y. Y. Xia, *Adv Funct Mater*, 2007, 17, 3877-3884.
3. M. Zhou, L. Liu, L. Yi, Z. Yang, S. Mao, Y. Zhou, T. Hu, Y. Yang, B. Shen and X. Wang, *Journal of Power Sources*, 2013, 234, 292-301.
4. L. Liu, M. Zhou, G. Wang, H. Guo, F. Tian and X. Wang, *Electrochimica Acta*, 2012, 70, 136-141.
5. I. D. Gimenez, I. O. Mazali and O. L. Alves, *J Phys Chem Solids*, 2001, 62, 1251-1255.
6. C. M. Burba and R. Frech, *Solid State Ionics*, 2006, 177, 1489-1494.
7. R. Ramaraghavulu and S. Buddhudu, *Ceram Int*, 2011, 37, 3651-3656.
8. J. C. Yu, L. Z. Zhang, Z. Zheng and J. C. Zhao, *Chem Mater*, 2003, 15, 2280-2286.
9. W. Y. Wu, T. W. Shih, P. Chen, J. M. Ting and J. M. Chen, *J Electrochem Soc*, 2011, 158, K101-K106.